# UNIVERSITY OF OSLO
## DEPARTMENT OF PHYSICS

**Measurement of the $\tau$ Leptonic Branching Fractions in DELPHI**

**Mogens Dam**

Department of Physics
University of Oslo, Box 1048
N-0316 Oslo 3, Norway

UIO/PHYS/94-21
ISSN-0332-5571

Received: 1994-11-16

# REPORT SERIES

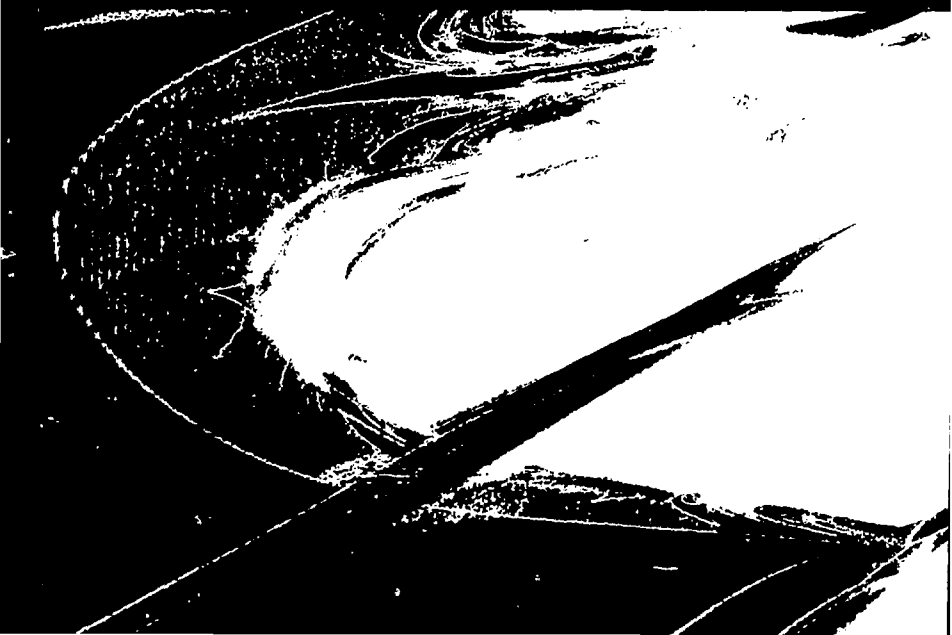

# Measurement of the $\tau$ Leptonic Branching Fractions in DELPHI

**Mogens Dam**

**Department of Physics**
**University of Oslo, Box 1048**
**N-0316 Oslo 3, Norway**

**UIO/PHYS/94-21** **Received: 1994-11-16**
**ISSN-0332-5571**

Presented at the Third Workshop on Tau Lepton Physics
(Montreux) - September 1994

# Measurement of the $\tau$ Leptonic Branching Fractions in DELPHI

Mogens Dam
University of Oslo
NORWAY

A preliminary measurement of the $\tau$ leptonic branching fractions from the DELPHI experiment at LEP is presented. The analysis is based on about 25,000 $Z^0 \to \tau^+\tau^-$ events observed in 1991 and 1992.

## 1. INTRODUCTION

Precise measurements of the branching fractions of tau decays to leptonic final states

$$\tau^- \to e^-\nu_\tau\nu_e \quad (1)$$

$$\tau^- \to \mu^-\nu_\tau\nu_\mu \quad (2)$$

can be used to test lepton universality in the charged weak current. In this report, new preliminary results on these decay modes are presented. The measurement is based on an analysis of about 25,000 $Z^0 \to \tau^+\tau^-$ events observed in the DELPHI detector at LEP in 1991 and 1992.

## 2. METHOD

The branching fraction for the decay of the tau to lepton $l$ was calculated according to the expression

$$B_l = \frac{N_l}{N_\tau}\frac{1-b_l}{1-b_\tau}\frac{1}{\epsilon_l^{\rm id}}\frac{\epsilon_\tau^{\rm sel}}{\epsilon_l^{\rm sel}}, \quad (3)$$

where $N_l$ is the number of identified leptons, $\epsilon_l^{\rm id}$ and $b_l$ the corresponding identification efficiency and background fraction, respectively; $N_\tau$ is the number of tau decays considered for identification, $b_\tau$ the corresponding background fraction; $\epsilon_l^{\rm sel}/\epsilon_\tau^{\rm sel}$ is the ratio of the tau selection efficiency for the decay channel $\tau \to l\nu\nu$ and the overall tau selection efficiency or in other words the relative enhancement of this decay mode due to the tau selection.

The selection of pure samples of leptonic tau decays proceeded in three stages. Firstly, a reference sample of $Z^0$ decays to tau pairs was selected. Secondly, strict channel specific requirements on the hemisphere opposite to the one considered for identification greatly reduced harmful backgrounds. Finally, the leptonic decays were identified.

The performance of the identification procedures was checked extensively not only using Monte Carlo simulation but as far as possible using physics channels well identified in the data from kinematic constraints. Examples of such channels were $Z^0$ decays to electron or muon pairs, and $\gamma\gamma$ interactions. Furthermore, the detector response to the various particle types was studied in detail by exploiting the redundancy existing between different components of the detector.

## 3. THE DELPHI DETECTOR AT LEP

The DELPHI detector and its performance is described in detail elsewhere [1]. Here a brief summary of the barrel part of the detector, defined as the polar angular region satisfying $|\cos\theta| < 0.731$, is presented.

### 3.1. Tracking

The principal device for the reconstruction of charged particle trajectories in the 1.2 Tesla magnetic field was the Time Projection Chamber (TPC) extending radially from 32 to 116 cm. The information from the TPC was supplemented by very precise space point information from a three layer silicon microstrip vertex detector (VD) at radii between 6 and 11 cm and from a cylindrical drift chamber (ID) positioned between the VD and the TPC. Located outside the Ring Imaging Cherenkov counter (RICH) at a radius of 205 cm, the Outer Detector (OD), consisting of five layers of drift tubes, provided a precise measurement of

the azimuthal coordinate. The measured momentum resolution was $\delta p/p^2 = 8 \times 10^{-4}$ GeV$^{-1}$.

### 3.2. Calorimetry

The High-density Projection Chamber (HPC) provided high granularity information on electromagnetic showers. Shower starting points were reconstructed with a precision better than 1 cm allowing a precise association of showers to charged tracks. The energy resolution was found to be $32\%/\sqrt{E(\mathrm{GeV})} \oplus 4.4\%$.

The Hadron Calorimeter (HCAL), consisting of streamer tubes interleaved with the iron of the magnet return yoke, provided an energy resolution for hadrons of about $140\%/\sqrt{E(\mathrm{GeV})}$. It was read out in 4 layers in depth with a granularity of about $3 \times 3$ degrees.

### 3.3. Particle Identification

In addition to the particle identification capabilities provided by the calorimetry, dedicated instrumentation for particle identification was available.

Whereas information from the RICH counters was not used in the analysis, extensive use was made of the measurement of the specific ionization in the TPC, which with up to 192 samples provided a $dE/dx$ measurement with 6.1% resolution, and of the information from the muon chambers providing three-dimensional information on muons penetrating the HCAL.

## 4. $\tau^+\tau^-$ REFERENCE SAMPLE

The decay of the $Z^0$ into a tau pair is characterized by two low multiplicity, highly collimated back-to-back jets consisting of charged and neutral particles. The undetected neutrinos from the tau decays lead to significant missing energy. These characteristics were exploited for the selection of a reference sample of tau pairs.

The DELPHI trigger system, which is based on highly redundant signals from various detector elements, provided a trigger efficiency of essentially 100% for tau pair final states.

As a initial step of the selection, events were separated into hemispheres by a plane perpendicular to the thrust axis, which was calculated using charged tracks. It was required that at least one of the two leading tracks (highest momentum track in a hemisphere) lie within the barrel region of the detector. Poorly reconstructed events were excluded by demanding at least one track per hemisphere. Most cosmic rays were rejected by requiring that both leading tracks had a point of closest approach to the center of the interaction region of less than 4.5 cm along the beam axis and of less than 1.5 cm in the plane perpendicular to the beam axis. Requiring additionally that the two leading tracks were separated by less than 3 cm along the direction of the beam axis at their closest approach to the interaction point exploited the timing information of the TPC to remove remaining cosmic ray events not arriving at the nominal collision time.

Table 1
Characteristics of the $\tau^+\tau^-$ reference sample

| | |
|---|---|
| Number of selected events | ~25,000 |
| Selection efficiency in $4\pi$ | 53% |
| Selection efficiency inside barrel | 82% |
| Backgrounds: Total | 2.8% |
| $e^+e^-$ & $(e^+e^-)e^+e^-$ | 1.8% |
| $\mu^+\mu^-$ & $(e^+e^-)\mu^+\mu^-$ | 0.5% |
| $q\bar{q}$ | 0.5% |

The majority of $Z^0$ decays to hadrons were removed by requiring a maximum of six charged tracks originating from the interaction region and a minimum angle between any two tracks in opposite hemispheres exceeding 160°. Two-photon events were excluded by requiring a total energy in the event (sum of neutral electromagnetic and charged energy) exceeding 8 GeV and a total transverse momentum of charged tracks exceeding 0.4 GeV.

Most decays of the $Z^0$ to $e^+e^-(\gamma)$ and $\mu^+\mu^-(\gamma)$ final states were excluded by requiring that the event acollinearity exceed 0.5° and that the two variables $p_{\mathrm{rad}} = \sqrt{p_1^2 + p_2^2}$ and $E_{\mathrm{rad}} = \sqrt{E_1^2 + E_2^2}$ both be less than the beam energy. Here the variables $p_{1(2)}$ and $E_{1(2)}$ were, for hemisphere 1 (2), the momentum of the leading track and the total electromagnetic energy inside a 30° cone about this track, respectively.

With an efficiency of 82% within the angular

acceptance, these criteria selected about 25,000 events from the 1991 and 1992 data. The total background of 2.8% was dominated by $Z^0$ decays into electron pairs which together with electron pairs from $\gamma\gamma$ collisions totaled 1.8%. At 0.5% muonic type backgrounds were less abundant. The main characteristics of the tau pair reference sample are summarized in Table 1.

## 5. THE DECAY $\tau \to e\nu\bar{\nu}$

### 5.1. Final tau decay sample

To be able to exclude as much of the background from $Z^0$ decays to electron pairs as possible, the leading track in both hemispheres was required to point to a region with good HPC performance. Following this, it was required that the total deposited energy in the hemisphere opposite to the one considered for identification did not exceed 36.5 GeV. In regions close to boundaries between HPC modules the energy deposited in the first layer of the HCAL was included in the sum of the electromagnetic energy.

Electron background from $\gamma\gamma$ interactions was effectively reduced by requiring the $dE/dx$ of the opposite hemisphere track to be inconsistent with that of an electron in events with only two charged tracks both softer than 9 GeV.

An optimal HPC performance for the electron identification was ensured by requiring the particle impact on the calorimeter surface to be further away than 0.5° from the center of an azimuthal boundary between HPC modules. It was furthermore asked that the ionization in the TPC was recorded by a minimum of 38 sense wires. This lead to a 4.1% loss of tracks around the boundary regions between the six azimuthal TPC sectors, and was well described by the Monte Carlo simulation.

Details of the selected tau decay sample are presented in Table 2. The selection procedure led to a relative suppression of the electron decay mode with respect to the overall sample of $0.75 \pm 1.20\%$. The dominant contribution to the uncertainty resulted from the loss of tracks close to the boundaries between TPC sectors. This turned out to be slightly larger for electrons than for other particles. The uncertainty was estimated from the stability of the identified electron fraction when the difficult regions were excluded and from a separate study of badly measured tracks.

Table 2
Final sample for $\tau \to e\nu\nu$ study

| | |
|---|---|
| Number of $\tau$ decays | 31,325 |
| $4\pi$ selection efficiency | 34.8% |
| $\epsilon_e^{sel}/\epsilon_\tau^{sel}$ | $99.25 \pm 1.20\%$ |
| Backgrounds: Total | $1.31 \pm 0.40\%$ |
| $e^+e^-$ | $0.19 \pm 0.12\%$ |
| $(e^+e^-)e^+e^-$ | $0.05 \pm 0.02\%$ |

### 5.2. Electron Identification

The main ingredients for the electron identification were $dE/dx$, the ionization measurement in the TPC, and $E/p$, the ratio between the electromagnetic energy deposition in the HPC and the track momentum. For both quantities pull variables were constructed based on the measured value of the variable in question, its resolution, and its expectation based on the electron hypothesis. The pull variables, $H_{dE/dx}^e$ and $H_{E/p}^e$, respectively, were defined as the signed number of standard deviations by which the measured value differed from its expectation. For $dE/dx$ use was made also of $H_{dE/dx}^\pi$, the pull variable based on the pion hypothesis.

For a tau decay to be identified as an electron it was required that the hemisphere contained a single charged track with momentum exceeding 0.46 GeV. As an initial step of the identification $dE/dx$ was asked to be compatible with that of an electron by requiring that $H_{dE/dx}^e$ be greater than $-2$. This reduced significantly the background from hadrons and muons, especially at low momentum, with a very low loss of signal. A high identification efficiency over the whole momentum range was ensured by a logical OR of two independent selection criteria based on $E/p$ and $dE/dx$, respectively:

- Particles with momentum greater than 2.3 GeV which deposited an electromagnetic energy matching the track momentum were retained as electron candidates. To al-

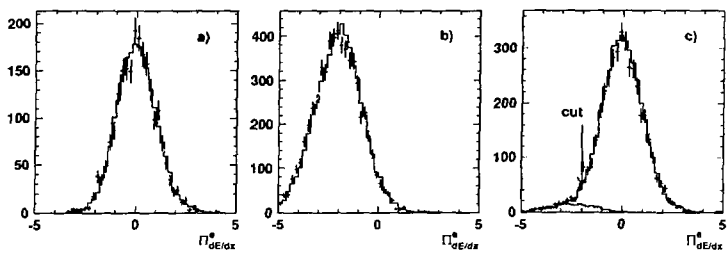


Figure 1. Pull variable $\Pi^{e}_{dE/dx}$ for a) electron test sample, b) hadron test sample, and c) after all other electron identification criteria had been applied. Points with error bars show real data. The full line shows the simulated data. The hatched area shows the background from hadronic tau decays.

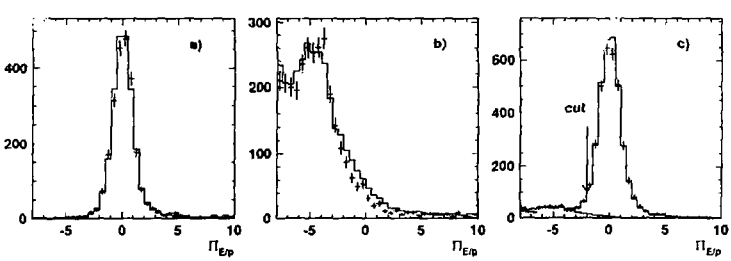


Figure 2. Pull variable $\Pi_{E/p}$ for a) electron test sample, b) hadron test sample, and c) after all other electron identification criteria had been applied. The discrepancy in the HPC response to hadrons is clearly visible. Points with error bars show real data. The full line shows the simulated data. The hatched area shows the background from hadronic tau decays.

low for additional energy deposited by photons, candidates were retained even if the energy exceeded the track momentum. It was required that $\Pi_{E/p} > -2$.

- Particles with momentum less than 23 GeV which left an ionization clearly exceeding that of a massive particle like a hadron or a muon were retained as electron candidates. It was required that $\Pi^{e}_{dE/dx} > 3$.

To reduce a residual background from hadronic tau decays, candidates with associated energy beyond the first HCAL layer were excluded. Furthermore, it was required that no electromagnetic neutral inside a 18° cone around the track had an energy exceeding 4 GeV. Neutral showers situated in the track plane on the outside of the track curvature were assumed to originate from bremsstrahlung and were excluded from this re-

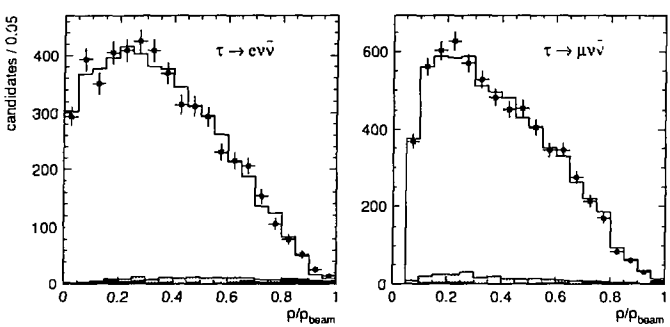


Figure 3. Momentum spectra of identified decays. Points with error bars show the real data. The full histogram shows the simulated data with mis-identified hadronic tau decays and backgrounds from non-tau sources shown in light and dark hatched, respectively.

quirement.

The performance of the identification criteria were studied in detail using test samples from the data. The efficiency at the higher and lower momentum regions was obtained from samples of electron pairs from $Z^0$ decays and $\gamma\gamma$ collisions, respectively. In the intermediate momentum region, the redundancy between the $dE/dx$ and the $E/p$ identification criteria enabled a precise determination of the efficiency of each of the two. The combination of these to get the overall efficiency relied on the assumption - confirmed by the simulation - that the $dE/dx$ and $E/p$ identification criteria were uncorrelated from an instrumental point of view. The probability for misidentifying a hadron as an electron was likewise estimated by exploiting the redundancy between $dE/dx$ and the calorimetry. In addition, extensive use was made of a test sample of hadron tracks from tau decays to $\rho$ and $a_1$ final states, which were selected by tagging $\pi^0$'s in the HPC. A discrepancy was found in the response of the HPC to hadrons between the simulated and the real data. The background estimate from the simulation was corrected correspondingly and an appropriate systematic uncertainty assigned.

Figures 1 and 2, respectively, show the pull variables $\Pi^e_{dE/dx}$ and $\Pi_{E/p}$ for test samples of electrons and hadrons. Apart from the mentioned discrepancy in $E/p$ for hadrons, good agreement was found between real and simulated data. Also shown are the two variables after all other identification cuts had been applied.

The background from electron pairs was estimated from a study of events with identified electrons in both hemispheres. This and a visual scan of events in which the electron candidate momentum exceeded 36.5 GeV showed that the Monte Carlo simulation underestimated the background from $Z^0$ decays to electron pairs by about a factor two. The background from $\gamma\gamma$ interactions was well described by the simulation.

With an efficiency of $90.92 \pm 0.93\%$ and a total background of $3.46 \pm 0.87\%$ of which $2.15 \pm 0.50\%$ were from hadronic tau decays and $1.31 \pm 0.71\%$ from non-tau sources, mainly $e^+e^-$ final states, 5059 electron candidates were identified. The momentum spectrum of the identified decays is shown in Figure 3. Good agreement with the simulated data, which is also shown, was observed.

## 6. THE DECAY $\tau \to \mu\nu\bar{\nu}$

### 6.1. Final tau decay sample

The background from final state muon pairs *remaining after the preselection was reduced* by a set of criteria based on a loose muon tagging in the hemisphere opposite to the one considered for identification. Any track seen in the muon chambers or in the outer layer of the hadron calorimeter was considered a loose muon candidate. Given a loose muon candidate in the opposite hemisphere it was required that i) its momentum was less than 32 GeV and ii) the momentum of the track considered for identification was less than 36.5 GeV. The second criterion, which was aimed at reducing the background from radiative $Z^0$ decays, produced a well understood step in the muon selection efficiency.

Muon background from $\gamma\gamma$ interactions was reduced by requiring, in the case of a loose muon candidate in the opposite hemisphere, at least one track in the event with momentum exceeding 9 GeV.

The cosmic ray background was significantly reduced by a tightening of the vertex constraints described in Section 4. It was required that at least one of the two leading tracks had a point of closest approach to the center of the interaction region of less than 0.3 cm in the plane perpendicular to the beam axis. Furthermore, in events with a single charged track in both hemispheres, the two tracks were required to be separated by less than 2 cm along the beam direction at their point of closest approach to the interaction region.

Finally, to ensure optimal detector performance, the track considered for identification was required to lie within the polar angular region given by $0.035 < |\cos\theta| < 0.731$.

Details of the selected tau sample are presented in Table 3. The selection procedure led to a relative enhancement of the muon decay channel with respect to the overall sample of $7.71 \pm 0.88\%$. Here the uncertainty from track losses was much smaller than in the electron case. Other contributions were estimated by considering the uncertainties in scale and resolution of the variables entering into the definition of the sample.

Table 3
Final sample for $\tau \to \mu\nu\nu$ study

| | | |
|---|---|---|
| Number of $\tau$ decays | | 41,122 |
| $4\pi$ selection efficiency | | 47.5% |
| $\epsilon_\mu^{\rm sel}/\epsilon_\tau^{\rm sel}$ | | $107.71 \pm 0.88\%$ |
| Backgrounds: | Total | $1.87 \pm 0.62\%$ |
| | $\mu^+\mu^-$ | $0.07 \pm 0.03\%$ |
| | $(\mu^+\mu^-)\mu^+\mu^-$ | $0.04 \pm 0.01\%$ |
| | Cosmic rays | $0.04 \pm 0.01\%$ |

### 6.2. Muon identification

For a tau decay to be identified as a muon it was required that the hemisphere contained a single charged track with momentum exceeding 3 GeV. The latter requirement was necessary in order to make sure a muon would penetrate through the HCAL to the muon chambers and thus allow identification. For the identification of the particle as a muon it was asked that it was observed in the muon chambers or in the outer layer of the HCAL. Further rejection of hadronic tau decays penetrating deep into the HCAL was ensured by asking the energy deposition in the HCAL to be consistent with that of a minimum ionizing particle; it was required that the average HCAL energy deposition per active layer did not exceed 3 GeV. With a very modest loss of efficiency this requirement *removed about two thirds of the remaining background*. Hadronic tau decays in which an isolated charged hadron was accompanied by one or more $\pi^0$'s or interacted in the HPC were further excluded by requiring a maximum of 1 GeV neutral electromagnetic energy inside a 18° cone around the charged track and a maximum of 3 GeV electromagnetic energy associated to the track.

The study of the identification criteria followed closely the procedure outlined for the electron channel. At the higher and lower momentum regions the efficiency was obtained from samples of muon pairs from $Z^0$ decays and $\gamma\gamma$ collisions, respectively. From the tau data themselves, a clean muon sample was selected by strict requirements on the observed hit pattern in the muon chambers only. From this sample the efficiency of all identification criteria except the one involving the *muon chambers was obtained*. *Since the muon*

Table 4
Statistics, efficiencies and backgrounds. The notation corresponds to that of Equation 1.

| | $\tau \to e\nu\bar{\nu}$ | $\tau \to \mu\nu\bar{\nu}$ |
|---|---|---|
| $N_\tau$ | 31,325 | 41,122 |
| $\epsilon_l^{sel}/\epsilon_\tau^{sel}$ | $0.9925 \pm 0.0120$ | $1.0771 \pm 0.0088$ |
| $b_\tau$ | $0.0131 \pm 0.0040$ | $0.0187 \pm 0.0062$ |
| $N_l$ | 5,059 | 6,586 |
| $\epsilon_l^{id}$ | $0.9092 \pm 0.0093$ | $0.8554 \pm 0.0075$ |
| $b_l$ | $0.0346 \pm 0.0087$ | $0.0392 \pm 0.0046$ |

chamber efficiency was found to be constant over the whole momentum range, the overall efficiency could thus be obtained. The probability for misidentifying a hadron as a muon was obtained from the previously mentioned test sample of charged hadrons from tau decays, which were selected by tagging $\pi^0$'s in the HPC.

The cosmic ray background remaining in the identified sample was estimated by an interpolation of the rate from outside the tight vertex cuts. Backgrounds from muon pairs were found to be well described by the simulation.

With an efficiency of $85.54 \pm 0.75\%$ and a total background of $3.92 \pm 0.46\%$ of which $3.20 \pm 0.40\%$ were from hadronic $\tau$-$a$ decays and $0.72 \pm 0.22\%$ were from non-tau sources, 6586 muon candidates were identified. The momentum spectrum of the identified decays is shown in Figure 3. Good agreement with the simulated data was observed.

The largest single drop in efficiency arose from the requirement that the track momentum exceeded 3 GeV necessary in order to ensure that the muon would penetrate to the muon chambers. The identification efficiency for tracks satisfying this requirement was $94.54 \pm 0.72\%$.

## 7. RESULTS

The leptonic branching fractions were derived from the main figures of the analysis summarized in Table 4

$$B_e = 17.51 \pm 0.23\ (\text{stat}) \pm 0.31\ (\text{syst})\ \% \quad (4)$$

$$B_\mu = 17.02 \pm 0.19\ (\text{stat}) \pm 0.24\ (\text{syst})\ \% \quad (5)$$

Table 5
Summary of relative uncertainties (in %)

| | $\tau \to e\nu\bar{\nu}$ | $\tau \to \mu\nu\bar{\nu}$ |
|---|---|---|
| Statistics | 1.29 | 1.13 |
| Tau selection | 1.21 | 0.82 |
| Non-$\tau$ background | 0.70 | 0.65 |
| Identification efficiency | 1.02 | 0.87 |
| Internal background | 0.51 | 0.41 |
| Total systematics | 1.80 | 1.42 |

A breakdown of the systematic uncertainties is presented in Table 5. The uncertainty of the tau polarisation in $Z^0$ decays was found to have a negligible effect. The results are in agreement with the current world average values [2]. They also agree with previously published results from DELPHI based on data from 1990 [3] but are more precise by a factor 2.7.

A test of e $\mu$ universality in the charged weak current can be performed from the ratio of the muon and electron branching fractions

$$\frac{B_\mu}{B_e} = 0.9720 \pm 0.017\ (\text{stat}) \pm 0.020\ (\text{syst}). \quad (6)$$

Here a 20% correlation of the systematic uncertainties, arising from the tau selection and the non-tau background, has been accounted for. The result is in excellent agreement with the theoretical expectation of 0.9726, where the small excursion from unity is due to the mass of the muon. Expressed in terms of the $Wl\nu_l$ couplings the result reads

$$\frac{g_\mu}{g_e} = 0.9997 \pm 0.0131. \quad (7)$$

Assuming e $\mu$ universality the exclusive branching fraction results can be combined to obtain the average massless leptonic branching fraction

$$B_l = 17.50 \pm 0.15\ (\text{stat}) \pm 0.20\ (\text{syst})\ \% \quad (8)$$

Combining this result with the current DELPHI measurement of the tau lifetime [4] $\tau_\tau = 295.2 \pm 4.2$ fs allows a test of $\mu$ - $\tau$ universality in the charged weak current based on the relation

$$\left(\frac{g_\tau}{g_\mu}\right)^2 = 0.9998 \cdot \frac{\tau_\mu}{\tau_\tau}\left(\frac{m_\mu}{m_\tau}\right)^5 B_l \quad (9)$$

Here the numeric factor deviates slightly from unity due to radiative effects and due to the finite mass of the W boson [5]. Using the new very precise BES determination of the tau mass $m_\tau = 1776.96^{+0.27}_{-0.25}$ MeV/$c^2$ presented at this conference [6] it is found that

$$\frac{g_\tau}{g_\mu} = 0.9837 \pm 0.0097, \qquad (10)$$

where the uncertainty is composed of equally large contributions from the lifetime and the branching fraction measurements, and where the uncertainty from the tau mass is by now negligible. The small deviation from universality of about 1.7 standard deviations cannot be considered significant and is not generally confirmed by other experiments [7].

## ACKNOWLEDGEMENTS

I would like to thank my DELPHI colleagues, especially Martin McCubbin, who contributed to the achievement of the presented results. In addition I would like to thank the organizers of the workshop for a very pleasant physics conference.

This work was supported in part by a grant from the Norwegian Research Council.

## REFERENCES

1. The DELPHI Collaboration, P. Aarnio *et al.*, Nucl. Instr. & Meth. **A303** (1991) 233.
2. Particle Data Group, Phys. Rev. **D50** (1994) 1173.
3. The DELPHI Collaboration, P. Abreu *et al.*, Z. Phys. **C55**, 555 567 (1992).
4. The DELPHI Collaboration, P. Abreu *et al.*, Phys. Lett. **B302** (1993) 356.
   The publication, based on 1991 data, was updated by preliminary 1992+1993 results for this conference. For details see A. Andreazza and I. Ferrante, these proceedings.
5. W J. Marciano and A. Sirlin, Phys. Rev. Lett **D48**, 307.
6. Qi Nading, these proceedings.
7. M Davier, these proceedings.

| FYSISK INSTITUTT<br>FORSKNINGS-GRUPPER | DEPARTMENT OF PHYSICS<br>RESEARCH SECTIONS |
|---|---|
| Biofysikk | Biophysics |
| Elektronikk | Electronics |
| Elementærpartikkelfysikk | Experimental Elementary Particle Physics |
| Faste stoffers fysikk | Condensed Matter Physics |
| Kjerne- og energifysikk | Nuclear and Energy Physics |
| Plasma- og romfysikk | Plasma and Space Physics |
| Strukturfysikk | Structural Physics |
| Teoretisk fysikk | Theoretical Physics |